PHILOSOPHICAL TRANSACTIONS OF THE ROYAL SOCIETY A
MATHEMATICAL, PHYSICAL & ENGINEERING SCIENCES

Time-scales of magma formation, ascent and storage beneath subduction-zone volcanoes

S. P. Turner, R. M. M. George, P. J. Evans, C. J. Hawkesworthy and G. F. Zellmery

Phil. Trans. R. Soc. Lond. A 2000 **358**, 1443-1464
doi: 10.1098/rsta.2000.0598

THE ROYAL SOCIETY

Time-scales of magma formation, ascent and storage beneath subduction-zone volcanoes

By S. P. Turner†, R. M. M. George†, P. J. Evans, C. J. Hawkesworth† and G. F. Zellmer†

Department of Earth Sciences, The Open University, Milton Keynes MK7 6AA, UK

There is now sufficient information to attempt an integrated model for melt generation, transfer and storage beneath subduction-zone volcanoes. Fluid release from the subducting oceanic crust into the mantle wedge may occur over a period ranging from a few hundred kyr, to as little as less than 1 kyr, before eruption. This supports models in which fluid addition is closely linked to partial melting, though there may also be evidence for a component of decompression melting. The timing of the onset of fluid addition may be linked to the rate of subduction (i.e. water supply rate) and the angle of subduction, and, consequently, the thermal structure of the mantle wedge. In contrast, contributions from subducted sediments to subduction-zone lava sources appear to occur some 350 kyr–4 Myr before eruption. Evidence for partial melting of the sediment component, combined with the short fluid transfer times, phenocryst equilibration temperatures and other observations all point to quite high mantle wedge temperatures close to the interface with the subducting plate. New ^{226}Ra data permit only a short period of time between fluid addition and eruption. This requires rapid melt segregation, magma ascent by channelled flow and minimal residence time within the lithosphere. Typically, the evolution from basalt to andesite occurs rapidly during ascent or in magma reservoirs, inferred from some geophysical data to lie within the lithospheric mantle. Mineral isochron data suggest that some andesitic magmas subsequently stall in more shallow crustal level magma chambers, where they can evolve to dacitic compositions via fractionation, typically combined with assimilation, on time-scales of a few thousand years or less.

Keywords: andesite; subduction zone; melt generation; magma ascent; crustal residence; time-scales

1. Andesites and subduction zones

Andesite is the predominant magma composition erupted from 61% of the world's subaerial volcanoes (Gill 1981). Most of these volcanoes are associated with subduction zones, and magmatism in this tectonic setting constitutes *ca.* 15% (0.4–0.6 km^3 yr^{-1}) of the total global output (Crisp 1984). The composition of the continental crust is also broadly andesitic, and subduction zones were therefore once postulated to be the main site of continental crust generation (Taylor & McLennan 1981). It is now known that andesites are rarely primary magmas but, rather, the

† Present address: Department of Earth Sciences, University of Bristol, Bristol BS8 1RJ, UK.

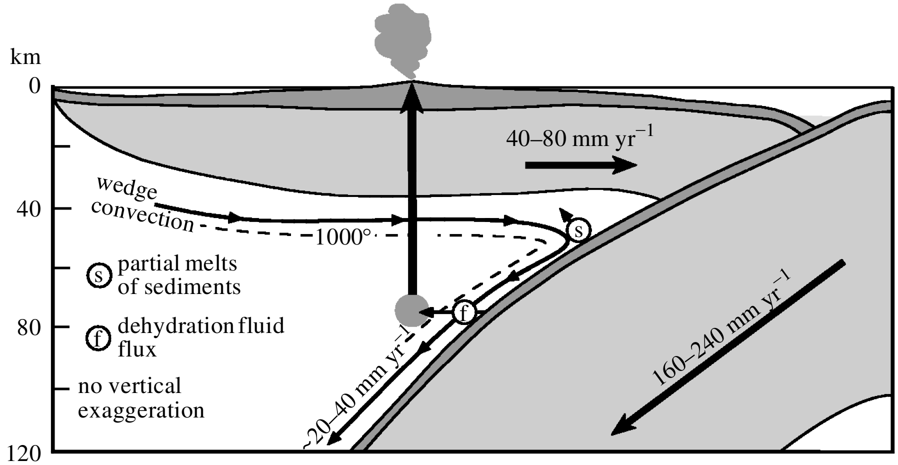

Figure 1. Scaled cross-section of the Tonga–Kermadec subduction zone, illustrating the inferred mantle wedge dynamics and fluid fluxes (modified from Turner & Hawkesworth 1997).

differentiates of basaltic parental magmas produced by partial melting of peridotite (see the review by Grove & Kinzler (1986)), and the bulk flux from the asthenosphere to the lithosphere at subduction zones is basaltic not andesitic (Arculus 1981; Ellam & Hawkesworth 1988). Even though basalt is the input, andesite remains volumetrically the most dominant output from subduction-related volcanoes. Many subduction-zone volcanoes have been responsible for the most hazardous, historic volcanic eruptions (e.g. Mt Pelée, Tambora, Krakatau, Mt St Helens), and some individual arc volcanoes, such as Shiveluch in Kamchatka, have effusion rates as high as 0.005 km^3 yr^{-1} (Crisp 1984). Here, we review the available constraints on the time-scales of melt generation, transfer and storage beneath subduction-zone volcanoes. These provide important insights into the physical processes of magma formation, and may ultimately permit better prediction of eruptive hazards.

2. Subducted components and the time-scales of their transfer

The principal components of a subduction zone and the possible locations of various elemental fluxes in this tectonic environment are illustrated in figure 1. A distinctive geochemical signature of subduction-zone magmas (figure 2) is the enrichment in large-ion lithophile elements (LILEs) relative to high-field-strength elements (HFSEs) (see, for example, Gill 1981; Hawkesworth *et al.* 1997). Both the subducted altered oceanic crust and sediments are potential sources of this subduction component. Experimental data, however, suggest that the high LIL/HFSE ratios reflect the relative mobility and immobility (respectively) of these elements in the slab-derived fluids (see, for example, Brenan *et al.* 1995; Keppler 1996). Importantly, the highest LIL/HFSE ratios (e.g. Ba/Th) are found in those rocks with the lowest $^{87}Sr/^{86}Sr$ and $^{206}Pb/^{204}Pb$ ratios, and from this it has been inferred that the fluid end-member was derived from the subducting altered oceanic crust rather than the overlying sediments (Miller *et al.* 1994; Turner *et al.* 1996; Turner & Hawkesworth 1997). Additionally, the presence of ^{10}Be and negative Ce anomalies in some subduction-zone lavas can be taken as unambiguous evidence for a contribution from subducted sediments (see,

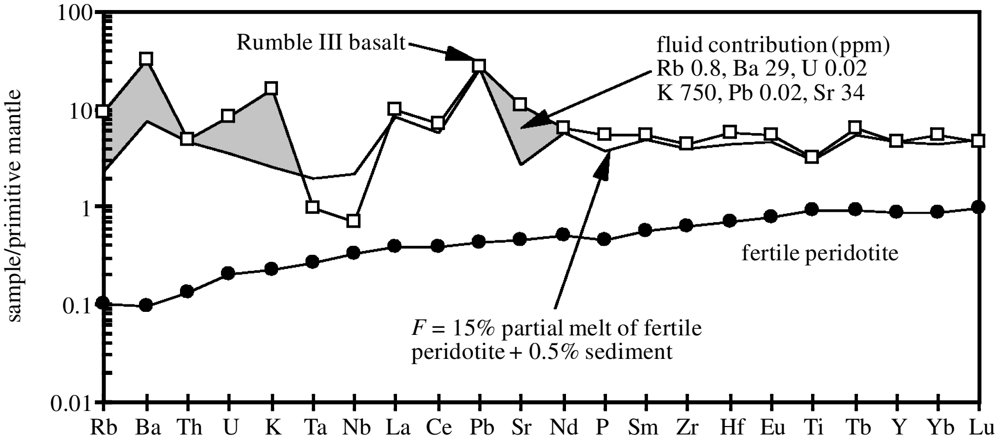

Figure 2. Primitive mantle-normalized incompatible trace-element diagram illustrating the three-component mass-balance model for a basalt ($SiO_2 = 51.7\%$) from the Rumble seamounts in the southern Kermadec island arc (after Turner *et al*. 1997). The solid line without symbols represents a 15% partial melt of a source composed of the fertile peridotite source shown, to which 0.5% sediment was added. The resultant model composition provides a reasonable match to the Th, rare earth element, Zr, Hf and Ti contents of the basalt. The overestimate of the Ta and Nb concentrations in the model peridotite + sediment melt is one line of evidence that the sediment component is transferred as a partial melt (assumed to be formed in the presence of residual rutile that retains Ta and Nb). The excesses of Rb, Ba, U, K, Pb and Sr in the basalt are attributed to fluid addition (shaded area; composition indicated in ppm) to the source.

for example, Hole *et al*. 1984; Morris *et al*. 1990). Thus, most recent studies have argued for a three-component model (figure 2) in which separate contributions from the mantle wedge, the slab fluid and the sediment have been identified (see, for example, Kay 1980; Ellam & Hawkesworth 1988; Miller *et al*. 1994; Turner *et al*. 1996, 1997; Elliott *et al*. 1997; Hawkesworth *et al*. 1997).

(*a*) *Transfer of the sediment component*

Several studies have found evidence that the sediment component (as identified from negative Ce anomalies, elevated Th/Ce ratios and unradiogenic $^{143}Nd/^{144}Nd$) is characterized by fractionated U/Th, Nd/Ta and Th/Nb ratios and so it has been suggested that the sediment component is transferred as a partial melt formed in the presence of a residual phase(s) that retains HFSE (see figure 2, Elliott *et al*. (1997) and Turner & Hawkesworth (1997)). Because the sediment component requires a fractionated U/Th ratio yet appears to be in U–Th isotope equilibrium, Elliott *et al*. (1997) have argued for the Marianas arc that transfer of this component from the subducting plate must have occurred at least 350 kyr ago. In north Tonga, Turner & Hawkesworth (1997) used identification of the Louisville volcaniclastic sediment signature to estimate a sediment component transfer time of 2–4 Myr. Thus, although these models require testing, there is growing evidence that the contributions from the subducted sediment are (a) partial melts, and (b) occur some 350 kyr–4 Myr before fluid addition (see below).

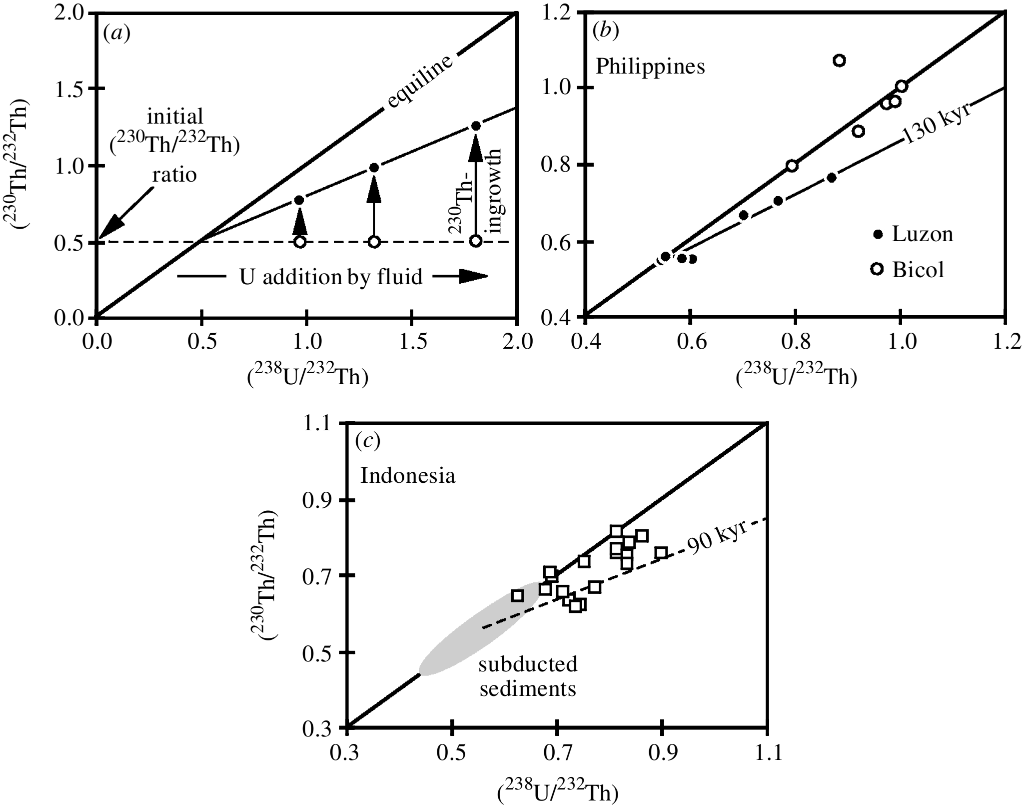

Figure 3. (*a*) Schematic equiline diagram illustrating U–Th isotope systematics with examples from (*b*) the Philippines (data from McDermott & Hawkesworth 1991; McDermott *et al*. 1993) and (*c*) Indonesia (S. P. Turner, unpublished data). One lava with excess ^{230}Th lies to the left of the equiline in (*b*), possibly due to the presence of residual garnet or aluminous clinopyroxene during partial melting.

(*b*) *Transfer of the fluid component*

Disequilibria between the short-lived nuclides of the U-series decay chain (U–Th–Pa–Ra) record fractionation on time-scales of less than 350 000 years, and, whereas Th and Pa behave as relatively immobile HFSEs, U and Ra are predicted to be highly mobile in oxidizing aqueous fluids (Brenan *et al*. 1995; Keppler 1996). Thus, fluids produced by dehydration reactions in the subducting, altered oceanic crust selectively add U (along with other fluid mobile elements) to the mantle wedge. So long as this is the principal cause of U/Th fractionation in whole rocks, U–Th isotopes can be used in the study of young lavas to estimate the time elapsed since fluid release into the mantle wedge. Firstly, U and Th have similar and small distribution coefficients in most minerals and so neither partial melting nor crystal fractionation is likely to have much effect on U/Th ratios. Secondly, crustal materials have low U/Th ratios and so crustal contamination would act to reduce the U/Th ratio. Therefore, the high U/Th ratios observed in the vast majority of arc lavas are generally accepted to reflect high U/Th ratios in the mantle source due to U addition by fluids from the subducting

Table 1. *Time elapsed since U fluid flux beneath subduction zones*

subduction zone	^{238}U–^{230}Th age (kyr)	reference
intra-oceanic arcs		
Tonga	60	Turner *et al.* (1997)
Kermadec	60	Turner *et al.* (1997)
Marianas	30	Elliott *et al.* (1997)
Philippines	130	McDermott *et al.* (1993)
Lesser Antilles	90	Turner *et al.* (1996)
Aleutians	<10	George *et al.* (1999)
New Britain	200	Gill *et al.* (1993)
South Vanuatu	59	Turner *et al.* (1999)
Central Vanuatu	16	Turner *et al.* (1999)
continental or transitional arcs		
South Chile	20	Sigmarsson *et al.* (1990)
New Zealand	60	Hughes (1999)
Kamchatka	>150	Turner *et al.* (1998)
Aegean	147	Zellmer *et al.* (2000)
Indonesia	>90	S. P. Turner (unpublished data)
Alaska	50	George *et al.* (1999)
Nicaragua	90	Reagan *et al.* (1994)

plate. In practice, information on the timing of fluid release can either be obtained from along-arc suites of lavas that form inclined arrays on U–Th equiline diagrams, or if the initial (^{230}Th/^{232}Th) ratio is constrained (figure 3*a*). For example, lavas from the Luzon arc in the Philippines scatter around a 130 kyr isochron (figure 3*b*). In contrast, lavas from the Java and Sunda sections of the Indonesian arc form a scatter on figure 3*c*, and, at best, a maximum transfer time can be obtained if the initial ratio is estimated from the composition of the subducting sediments. Finally, in the case of the Bicol arc east of the Philippines, analysed lavas lie within error of the equiline (figure 3*b*), and so either fluid addition did not result in U–Th disequilibrium in this instance or else the time since U addition is 350 kyr. In total, about 15 arcs have now been studied for U–Th disequilibria and the results are summarized in table 1, indicating that the time since U addition by fluids from the subducting oceanic crust appears to vary from 10 to 200 kyr before eruption. These variations can occur within the single arc due to the effects of tectonic collisions on the rate of subduction, such as occurs in New Britain (Gill *et al.* 1993) and Vanuatu (Turner *et al.* 1999), or possibly even through the life of a single volcano such as Santorini (Zellmer *et al.* 2000).

^{226}Ra has a much shorter half-life (1600 years) than its parent ^{230}Th (75 kyr) and so provides the opportunity to look at very recent fractionations of Ra/Th. Mass spectrometric measurements of (^{226}Ra/^{230}Th) are only just becoming available (figure 4); however, they confirm large ^{226}Ra excesses, indicated by earlier activity counting methods (Gill & Williams 1990). Turner & Hawkesworth (1997) speculated that ^{226}Ra excesses in subduction-zone lavas might have developed during partial

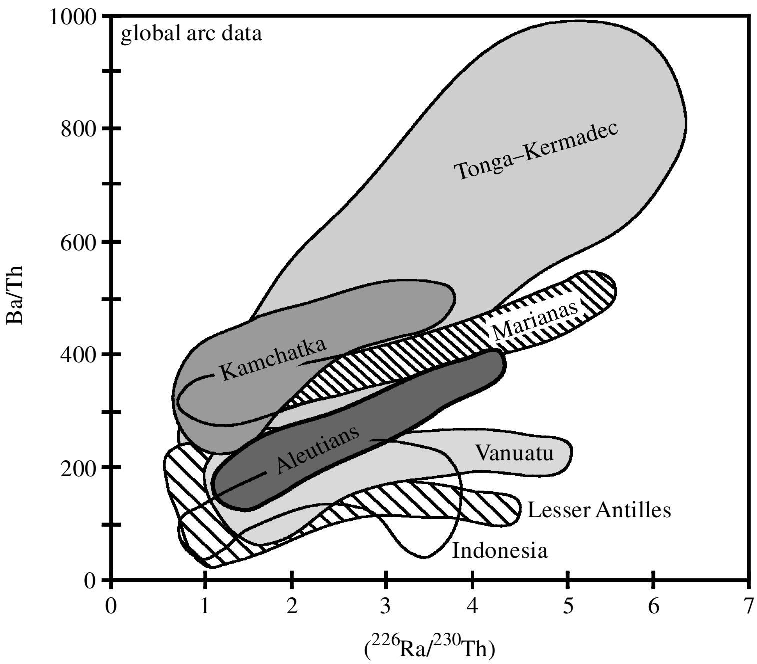

Figure 4. Ba/Th versus (^{226}Ra/^{230}Th) for the global arc data (S. P. Turner, unpublished data). The positive correlations with Ba/Th, which is sensitive to fluid additions (cf. figure 2), suggest that the observed ^{226}Ra excesses result from Ra addition by fluids from the subducting plate.

melting; however, the newly obtained data show that ^{226}Ra excesses are generally well correlated with Ba/Th (figure 4). Like U/Th, Ba/Th is unlikely to be fractionated during crystal fractionation and crustal materials have low Ba/Th ratios relative to most arc lavas. Moreover, the highest Ba/Th ratios occur in those arc rocks with the lowest ^{87}Sr/^{86}Sr ratios, and so the observed ^{226}Ra excesses are inferred to be a mantle signature resulting from fluid addition to the mantle wedge. At face value, the ^{226}Ra evidence for fluid addition in the last few thousand years appears to be inconsistent with the interpretation that U/Th disequilibria resulted from fluid addition 10–200 kyr ago (table 1). However, unlike U, ^{226}Ra lost to the mantle wedge during initial dehydration continues to be replenished in the subducting altered oceanic crust by decay from residual ^{230}Th (figure 5) on time-scales of tens of thousands of years, until all of the residual ^{230}Th has decayed away (350 kyr later). Thus, if dehydration reactions and fluid addition occur step-wise or as a continuum (Schmidt & Poli 1998), albeit over a short period of time, ^{226}Ra excesses will reflect the last increments of fluid addition, whereas U–Th isotopes record the time elapsed since the onset of fluid addition (see Turner *et al.* (2000) and also figure 5).

3. Causes and time-scales of melt generation and ascent

Subduction-zone magmatism is widely regarded to reflect partial melting caused by lowering of the peridotite solidus through addition of fluids released by dehydration reactions in the subducted altered oceanic crust (see, for example, Tatsumi *et al.* 1986; Davies & Bickle 1991). A strong dependence on fluid addition is consistent

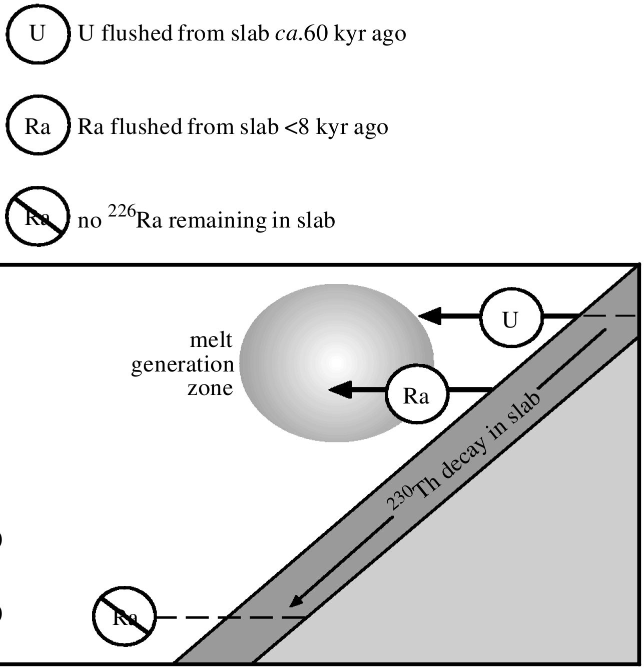

Figure 5. Illustration of progressive distillation of fluid mobile elements from the subducting plate (Turner *et al*. 2000). See text for explanation.

with the apparent correlation between volcanic output and rate of subduction from east to west along the Aleutian arc (Marsh 1987). Similarly, there is an absence of volcanism in South America above the area of subduction of the Chile ridge. This will be the hottest part of the wedge but also the driest, again suggesting that partial melting is fluid induced. However, the observation of eruption temperatures well in excess of the hydrous peridotite solidus and the occurrence of some essentially anhydrous arc magmas have been raised in objection to this hydrous fluxing model (Sisson & Bronto 1998). Additionally, several geochemical studies have argued that there is evidence for a component of decompression melting in arc lavas (Plank & Langmuir 1988; Pearce & Parkinson 1993). U-series isotope constraints can be used to provide independent information on the process of partial melting in the mantle wedge above subduction zones.

(*a*) *Hydrous fluxing*

The evidence that fluids were still being added to the mantle wedge less than a few thousand years before eruption (figure 4) strongly supports models in which fluid addition is closely linked to partial melting (figure 1). It has been suggested that fluid transfer occurs horizontally across the wedge by a series of hydration–dehydration reactions (Davies & Stevenson 1992). However, such a process would require fluid transfer time-scales of several Myr, which could only be reconciled if the observed U and Ra excesses were generated by the final amphibole dehydration reaction before melting (Regelous *et al*. 1997). However, Ba is more compatible than Th in amphibole (La Tourette *et al*. 1995), and so fluids produced in the presence of residual amphibole

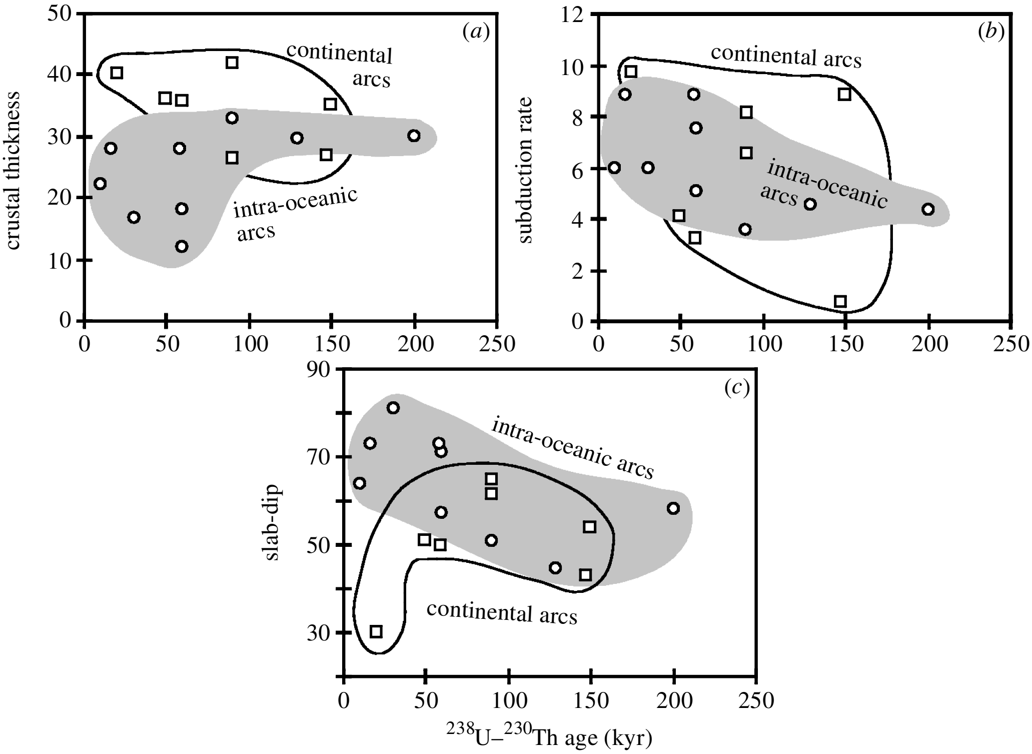

Figure 6. Plots of time since U fluid flux versus subduction-zone parameters for the world's arcs (deep slab dip and subduction rates taken from Jarrard (1986); crustal thicknesses from Gill (1981)).

would have low Ba/Th ratios and ($^{226}Ra/^{230}Th$) < 1 (assuming that Ra behaves similarly to Ba). Instead, those lavas with the strongest fluid signature (i.e. largest ($^{238}U/^{230}Th$) ratios) also have the highest Ba/Th ratios and the largest Ra excesses (figure 4), and that implies that amphibole is not a residual phase but melts out. By implication, the major U/Th and Th/Ra fractionation is inferred to occur during fluid release from the subducting plate, where redox conditions are the most strongly oxidizing. Thus, the combined U–Th–Ra isotope data are inconsistent with fluid transfer by a series of hydration–dehydration reactions, and would seem to require that fluid transfer occurs instead by hydraulic fracturing (Turner & Hawkesworth 1997; Davies 1999).

(b) *Links to physical parameters*

If the U–Th ages listed in table 1 are taken as the time elapsed between the onset of fluid addition (see above) and magma eruption, then there might be expected to be links between the variations in these ages and parameters that are sensitive to both the rate of fluid addition and the thermal structure of the mantle wedge. Heath *et al.* (1998) speculated whether the older U–Th ages simply reflected stalling of magmas within thicker crust, such that the transfer time within the wedge was relatively constant. However, as more data have been obtained, this appears not to be the case and figure 6*a* emphasizes that there appears to be no simple link between

U–Th age and crustal thickness. In figure 6*b*, *c*, the time since U addition from the subducting plate is plotted against subduction rate and dip of the subducting plate. Although there is significant scatter, there is some suggestion of a negative trend in both figures, most clearly apparent in the data from oceanic arcs. The rate of subduction will control the amount of water that is added to the mantle wedge over a given time (Davies & Stevenson 1992) and high rates may correspond to shorter time-scales of U transfer. If correct, it may be that the degree of partial melting and possibly melt rate will increase as a function of the amount of water added to the mantle source (Davies & Bickle 1991; Stolper & Newman 1994), both of which might result in shorter transfer times. Finally, temperatures in the mantle wedge at a fixed distance from the down-going plate will increase as the angle of subduction increases (Davies & Stevenson 1992). This leads to shorter distances that must be traversed by fluids or hydrated mantle before the amphibole peridotite solidus is encountered. In summary, although there may be good reasons why timing of the onset of fluid addition should in some way be linked to the rate of subduction (i.e. water supply rate) and the angle of subduction (i.e. the thermal structure of the mantle wedge), the data presently available provide only weak support for this.

(*c*) *Sediment addition and thermal structure in the wedge*

In contrast to the rapid fluid transfer time-scales, contributions from subducted sediments appear to have longer transfer times, and, accordingly, they are assumed not to be directly involved in triggering partial melting and volcanism. Nevertheless, thermal models for the mantle wedge and the down-going slab are very sensitive to whether this sediment component is transferred by partial melting or by tectonic delamination (mechanical mixing), and whether there are sediment contributions in the fluid component. As outlined above, at present the evidence is that the sediment component is transferred as a partial melt, and the Louisville volcaniclastic sediment signal in north Tonga has been used to argue that the transfer time of the sediment component into the arc magmas was 2–4 Myr (Turner & Hawkesworth 1997). Such long transfer times require the transfer of sediment into the mantle wedge at shallow levels (figure 1), and decoupling of convection in the wedge from the down-going plate in order to slow the transfer of the sediment component to the site of partial melting (Turner & Hawkesworth 1997). Partial melting of sediments at shallow levels requires temperatures of greater than 700 °C (Nichols *et al*. 1994; Johnson & Plank 1999), and, thus, a thermal structure in the mantle wedge several hundred degrees hotter than that predicted by current numerical thermal models (see, for example, Davies & Stevenson 1992). Higher wedge temperatures may help to reconcile the inferred high equilibration temperatures of some arc lavas (see, for example, Sisson & Bronto 1998).

(*d*) *A role for decompression melting?*

Although the preceding sections have concentrated on partial melting by hydrous fluxing, several studies have argued for a component of decompression melting in the production of arc lavas (Plank & Langmuir 1988; Pearce & Parkinson 1993; Sisson & Bronto 1998). In the first detailed study of ^{231}Pa–^{235}U disequilibria in subduction-zone lavas, Bourdon *et al*. (1999) showed that it is possible to distinguish elemental fractionation due to fluid addition from that produced during partial melting in the Tonga–Kermadec arc. Fluid addition results in (^{231}Pa/^{235}U) < 1, and this is preserved when partial melting causes little subsequent fractionation of Pa/U ratios. However, the more frequent observation in arc lavas is (^{231}Pa/^{235}U) ratios above 1, and this has been attributed to the effects of the partial melting process (Pickett & Murrell 1997; Bourdon *et al.* 1999). In mid-ocean ridge basalts, (^{231}Pa/^{235}U) ratios above 1 can be attributed to the effects of dynamic melting (see, for example, McKenzie 1985*b*); however, that requires partial melting on time-scales of tens of kyr. Such a model is unlikely to be applicable to subduction-zone melting because those time-scales would not preserve the observed ^{226}Ra excesses. Preliminary calculations suggest that the effects of equilibrium melt transport (Spiegelman & Elliott 1993), subsequent to the onset of partial melting that commences in response to hydrous fluxing, may be required to explain the observed ^{231}Pa excesses (Bourdon *et al.* 1999).

(*e*) *Melt segregation and ascent rates*

Theoretical calculations suggest that the segregation and ascent time-scales for basaltic magmas are likely to be short (McKenzie 1985*a*). One of the inescapable conclusions from the U-series disequilibrium data is that significantly less than a few half lives (i.e. 1600–3200 yr) can have elapsed since the generation of the ^{226}Ra excesses observed in the subduction-zone lavas plotted on figure 4. This is a key constraint and requires that segregation of the melt from its matrix and ascent occur on rapid time-scales. The transition from porous to channelled magma flow will be swift if melting rates are high, and the threshold porosity is quickly exceeded. If partial melting occurs at 80–100 km depth beneath subduction-zone volcanoes, then the required magma ascent rates are of the order of tens to hundreds of metres per year. In practice, ascent rates could be significantly faster and values as high as 1.8 km d^{-1} were estimated in Vanuatu (Blot 1972). These rising magmas initially traverse the inverted geothermal gradient in the lower half of the mantle wedge followed by the 'right-way-up' geotherm before encountering the base of the lithospheric mantle and the density change at the Moho, where they might be expected to slow or to stall and pond.

4. Residence times within the crust

U-series isotope data can also be used to assess the residence times of lavas, either from variations in lavas derived from a common parental magma (see, for example, Condomines *et al.* 1995), or, by inference, from mineral isochrons whose ages exceed eruption ages. Note that in order for mineral isochrons to provide estimates of magma residence times, it is important that the groundmass (or whole rock if the groundmass dominates the U–Th budget of the rock) also lies on the mineral isochron. Otherwise, mineral isochrons simply provide ages of crystallization, which could reflect incorporation or remelting of older cumulate or wall-rock materials into new magma batches (see, for example, Pyle *et al.* 1988; Sparks *et al.* 1990; Hughes & Hawkesworth 1999). The work of Zellmer *et al.* (2000) on Santorini provides an example of mineral isochrons whose ages appear to only slightly exceed eruption ages and for which the groundmass or whole rock lie on the isochron (figure 7). At present, such work is still largely in its infancy and table 2 summarizes the available results.

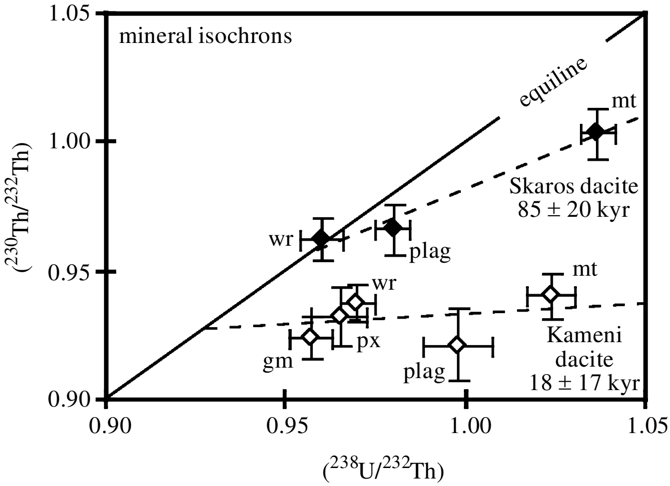

Figure 7. Examples of the use of U–Th mineral isochrons to infer crustal magma residence times from a study of Santorini by Zellmer *et al.* (2000). Two isochrons are shown, one from the 1940 Kameni dacite, yielding a pre-eruption age of *ca.* 18 kyr, and one from a 67 kyr-old dacite flow from the Skaros shield, which yields an age of 85 kyr, implying a pre-eruption age of 18 kyr. Note that for these two examples, the error bars allow that the isochrons could overlap with the eruption ages of these two lavas.

Because the isochrons listed in table 2 were determined on multiply saturated lavas in which plagioclase was a major phase, and because the groundmass or whole rock lie on the isochron in the majority of cases, they may well reflect residence times within the shallow arc crust. The results suggest that andesite residence times based on U–Th mineral isochrons range from 2 to 77 kyr. The Th–Ra mineral isochrons from the same rocks range from 0.5 to 8.2 kyr (table 2), although it should be noted that the whole-rock analyses lie above some of the Mt St Helens Th–Ra (but not U–Th) isochrons, and so those ages represent maximum residence times of magmas that may have mixed with older crystals (Volpe & Hammond 1991; Gardner *et al.* 1995). The longer half-life of ^{230}Th, however, means that analytical errors translate into larger uncertainties in isochron ages from the U–Th system compared with the Th–Ra system. Thus, the majority of the ages determined from the two systems agree within error. Exceptions include the Castle Creek andesite from Mt St Helens and the 1979 basaltic andesite from Soufrière (Upper Rabacca flow). The latter is known to contain excess ^{226}Ra (Chabaux *et al.* 1999), and there has been debate over some of these longer residence-time estimates and whether or not these may in part reflect incorporation of older cumulate materials (see, for example, Pyle *et al.* 1988; Sparks *et al.* 1990).

Constraints on magma residence times can be obtained in several other ways. The most straightforward is simply that the crustal residence time for magmas containing significant ^{226}Ra excesses cannot have been greater than 8000 years, so long as those ^{226}Ra excesses were produced in the mantle wedge (see above). For example, Condomines *et al.* (1995) used ^{230}Th–^{226}Ra disequilibria on whole rocks to infer that differentiation occurs on a short time-scale (200 years) at Mt Etna, with an upper limit of 1500 years for the residence time of the magma. In comparison, Pyle (1992) calculated steady-state magma residence times of 20–100 years for Etna, Strom-

Table 2. *Subduction-zone magma residence times (in kyr) from U-series isotope analyses of lava phenocrysts*

volcano	unit and bulk composition	$^{238}U–^{230}Th$ age	$^{226}Ra–^{230}Th$ age[a]	reference
Mt Shasta	Hotlum dacite	3 ± 18	7.3 ± 1.3	Volpe (1992)
	Hotlum andesite	28 ± 10	> 10	Volpe (1992)
	Hotlum andesite	27 ± 18	> 10	Volpe (1992)
	Black Butte dacite	13 ± 7	8.2 ± 2.1	Volpe (1992)
Mt St Helens	1982 dacite	6 ± 4	0.5	Volpe & Hammond (1991)
	Goat rocks andesite	4 ± 13	3	Volpe & Hammond (1991)
	Kalama andesite	2 ± 15	4.5	Volpe & Hammond (1991)
	Sugar bowl dacite	4 ± 3	1	Volpe & Hammond (1991)
	Castle Creek basalt	34 ± 16	5	Volpe & Hammond (1991)
	Castle Creek andesite	27 ± 12	< 10	Volpe & Hammond (1991)
Nevado del Ruiz	R0 andesite	7 ± 6	6.1 ± 0.5	Schaefer *et al.* (1993)
Soufrière	Waterloo andesite	74 ± 20	—	Heath *et al.* (1998)
	Soufrière Table b. andesite	77 ± 10	—	Heath *et al.* (1998)
	Upper Rabacca b. andesite	46 ± 27	< 10	Heath *et al.* (1998)
	Larikai andesite	56 ± 13	—	Heath *et al.* (1998)
Santorini	Skaros dacite	18 ± 20	—	Zellmer *et al.* (2000)
	Kameni dacite	18 ± 20	< 10	Zellmer *et al.* (2000)

[a] Inferred to be less than 10 kyr if ^{226}Ra disequilibria have been observed and greater than 10 kyr if not.

boli and Mt St Helens using whole-rock U-series isotope data. In the case of Etna, this estimate was similar to that obtained from magma output rates and estimated magma chamber volume. Note that in all of these studies, it is possible that phenocrysts within these lavas could be older than the estimated ages for the liquids. As an example of a technique for isolating the ages of minerals, Zellmer *et al*. (1999) have used Sr concentration profiles in plagioclase phenocrysts from the Kameni dacites, Santorini and the 1979 andesite from Soufrière on St Vincent in the Lesser Antilles, to estimate plagioclase residence times of 100–450 years.

In summary, estimates for the crustal residence times of andesite magmas are typically in the range of 50 to a few thousand years, although there is conflicting information in some instances. If mineral isochrons include recycled cumulate materials, then the ages obtained provide an upper limit for the magma residence time and important information on the time-scales of crystallization. The inferred short magma residence times can be viewed as being consistent with the overall picture from geophysical studies that crustal magma chambers beneath subduction-zone andesite volcanoes are likely to be small or absent. Numerous studies in the Cascades, Tonga and Vanuatu have consistently failed to find any evidence for their existence (see summaries by Gill (1981) and Iyer (1984)). Moreover, when crustal magma chambers have been observed beneath subduction-zone andesite volcanoes, they tend to be small (10^3 m in diameter) and shallow (typically 1–3 km in depth) and, by implication, transitory features (Iyer 1984; Marsh 1989; Dvorak & Dzurisin 1997). Thus, Gill (1981) concluded that if magma chambers exist, they are beneath dacitic to rhyolitic volcanoes. Certainly, calderas and granitic plutons provide undeniable evidence that large crustal magma chambers can form in subduction-zone terrains if magmas become sufficiently silicic and viscous. However, the reasons for the transition from short-lived and small andesitic chambers to large and possibly long-lived rhyolitic systems remain unclear. Moreover, those highly silicic systems may be characterized by magma residence times, which may reach orders of magnitude longer than those inferred for andesite magmas (see, for example, Halliday *et al*. (1989), but see also Sparks *et al*. (1990)).

5. Links to differentiation, assimilation and eruption

The mechanisms and time-scales by which magmatic evolution occurs are of great interest both from a petrological point of view and as a means of predicting eruptive hazards. By combining the U-series data in table 2 with other compositional data, it is just possible to make some preliminary statements about the time-scales of magmatic evolution, and to compare these with estimates from numerical models.

(*a*) *Time-scales of differentiation*

The crustal residence-time information (table 2) can be combined with geochemical data in order to place constraints on the time-scales of differentiation beneath andesite volcanoes. This discussion assumes that those isochrons provide residence-time information, and it is important to remember that these will be maximum magma residence times. In figure 8, we investigate these time-scales using MgO as the index of differentiation. Starting with the U–Th ages, although there is considerable scatter, the longer residence times tend to be associated with the more

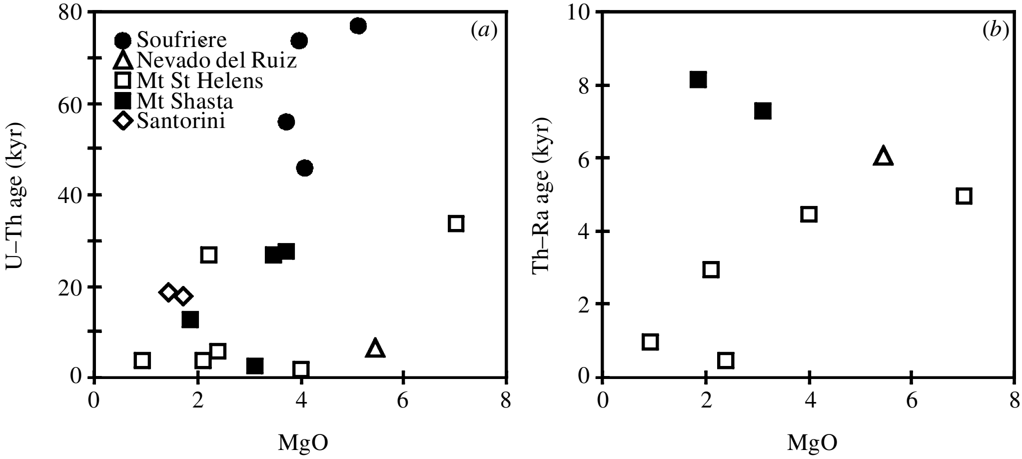

Figure 8. U–Th (*a*) and Th–Ra (*b*) mineral isochron ages from table 2 plotted against whole-rock MgO (see text for discussion).

primitive lavas, both in the overall data and for individual volcanoes (figure 8*a*). There are fewer Ra–Th ages (table 2); however, the data for Mt St Helens also show a positive correlation between Th–Ra age and MgO content (figure 8*b*). These relationships are consistent with, *but do not require*, evolution of a comagmatic set of lavas, where the more primitive lavas (and their phenocrysts), some portions of which have undergone fractionation, are older than their differentiated daughter products. As cautioned above, much care is required in drawing conclusions from these data, particularly given evidence for mixing with older minerals in some instances (Volpe & Hammond 1991; Gardner *et al*. 1995). However, taking the available data on face value suggests that a parental basaltic andesite magma batch can evolve to a system containing both andesite and some volume of daughter dacite, which requires some 50–80% fractional crystallization (Grove & Kinzler 1986), on time-scales of the order of less than 10^3 years. Despite the caveats mentioned above, such estimates are in good agreement with those predicted by numerical models for the cooling and crystallization of magma chambers, which predict magmatic evolution time-scales of the order of 10^2–10^3 years (see summary by Marsh 1989).

(*b*) *Time-scales of assimilation*

The more mafic lavas from intra-oceanic arcs often appear to have traversed the lithosphere without suffering significant crustal assimilation (see, for example, Elliott *et al*. 1997; Heath *et al*. 1998). Many other arc lavas show evidence for crustal assimilation, usually combined with crystal fractionation (see, for example, Davidson 1996; Zellmer *et al*. 2000). The time-scales for combined assimilation and differentiation have been estimated, using numerical thermal models, to be of the order of 10^2–10^3 years (Huppert & Sparks 1988; Edwards & Russell 1998), and these compare favourably with those determined from the residence-time estimates. The lavas erupted from Mt St Helens over the last few thousand years exhibit striking correlations between indices of assimilation and differentiation (Halliday *et al*. 1983) and the $^{87}Sr/^{86}Sr$ ratio–MgO correlation is reproduced in figure 9*a*. The correlation between magma residence time and MgO in figure 8*b* predicts a correlation between

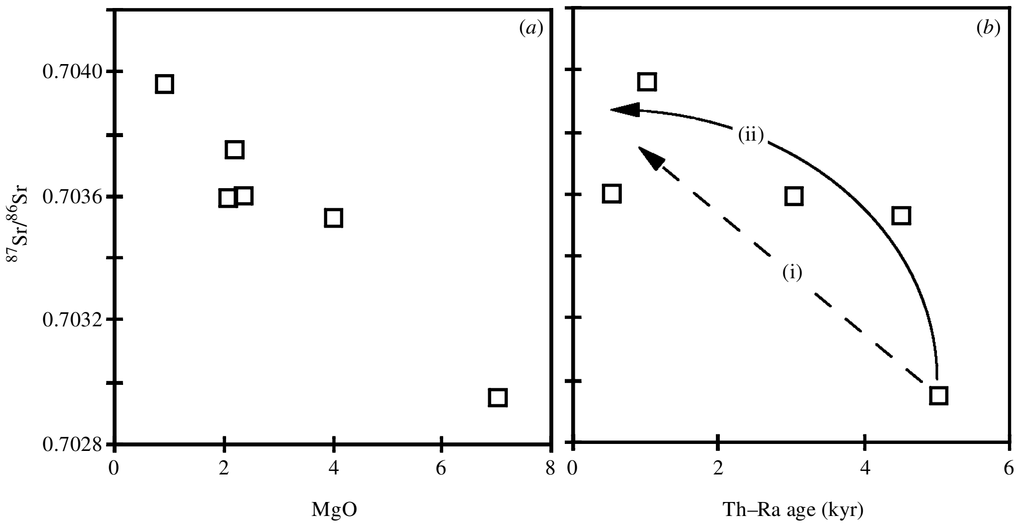

Figure 9. (*a*) Mt St Helens data (Halliday *et al.* 1983) showing the strong correlation between the $^{87}Sr/^{86}Sr$ ratio and MgO, which could be interpreted in terms of combined assimilation and fractional crystallization. (*b*) Probable correlation between the $^{87}Sr/^{86}Sr$ ratio and Th–Ra age (see text for discussion). Hypothetical paths illustrate how, with more data (*and evidence that mineral isochrons faithfully reflect magma residence times*), it might be possible to distinguish between systems where (i) assimilation was continuous, and (ii) assimilation was more efficient during the early stages of the system when magmas were hotter and more mafic.

residence time and $^{87}Sr/^{86}Sr$ ratio, and this is shown in figure 9*b*. *One* interpretation is that the younger, more-evolved liquids in this system are also the most contaminated (bearing in mind the caveats discussed above and that the $^{87}Sr/^{86}Sr$ ratio–MgO array may also reflect binary mixing). Certainly, assimilation will be most rapid during the early, hotter stages of magma evolution, but, unfortunately, there are not enough data to constrain whether the relationship in figure 9*b* is linear or curved. However, if it is linear, then a regression yields a rate of increase in the $^{87}Sr/^{86}Sr$ ratio of 0.0001 per thousand years. For comparison, Knesel *et al.* (1999) have recently presented Sr isotope profiles across sanidine phenocrysts that show an increasing $^{87}Sr/^{86}Sr$ ratio from core to rim, due to growth while country-rock assimilation was occurring. Sanidine growth rates are poorly constrained, however, using a *plagioclase* growth rate of 10^{-12} cm s^{-1} (Davidson & Tepley 1997); these data suggest a rate of increase in the $^{87}Sr/^{86}Sr$ ratio of 0.008 kyr^{-1}. This rate is higher than the estimate from Mt St Helens, but such phenocrysts may grow in the presence of large isotopic gradients at the margins of magma bodies where rapid cooling occurs (Wolff *et al.* 1999). Although the preceding discussion almost certainly represents an over-interpretation of a small set of data, the intention is simply to illustrate the *potential* information that could be obtained if the significance of U-series mineral isochrons can be properly established.

(*c*) *Links to eruptive mechanisms*

Numerous mechanisms have been proposed as the trigger for volcanic eruption, not least the decreases in density and volatile build-up that accompany magma differentiation (see, for example, Eichelberger & Westrich 1981; Tait *et al*. 1989; Cashman 1992; Sparks 1997). However, if the time-scales discussed above are in any way representative, they imply that there is no direct link between magma residence time and eruptive periodicity, since most andesite eruptions recur with a frequency of the order of tens to hundreds of years. Rather, eruptive periodicity may be linked to degassing (Jaupart 1996), and, for example, Tait *et al*. (1989) developed a model that predicted eruptive periodicity on the scale of years to hundreds of years due to crystallization-induced increases in volatile over-pressure. Conversely, some (Brophy *et al*. (1999) most recently) have argued that it is in fact vapour exsolution that induces shallow-level crystallization. Alternatively, eruption may be triggered by fresh, hot mafic inputs into existing magma chambers (see, for example, Sparks *et al*. 1977), and Sr isotope profiles in plagioclase phenocrysts provide impressive evidence that some magmatic systems suffered repeated recharge events (Davidson & Tepley 1997). Thus, in practice it appears that eruptive time-scales are typically shorter than those that can be resolved using ^{226}Ra–^{230}Th measurements. Detailed studies will require application of U-series nuclides with even shorter half-lives, such as ^{210}Pb (22 years) or ^{228}Ra (6 years). Few such measurements have been made on andesitic lavas, although Pyle (1992) estimated residence times of 11–89 years on the basis of reported data. Regarding the more hazardous subduction-zone volcanic eruptions, Gill (1981) observed that many andesite volcanoes erupt magmas that become more differentiated with time, often terminating with explosive eruptions of dacite. The data illustrated in figures 8 and 9 suggest that some dacitic magmas may take as long as several thousand years to be produced from basaltic–andesite parental magmas.

6. Towards a working model

So far this review has concentrated on the time-scales deduced from andesite magmas rather than their parental, basaltic magmas, which raises the question of the origin of andesite magma. Numerous detailed studies suggest that this evolution occurs at subcrustal depths (see, for example, Heath *et al*. 1998; Brophy *et al*. 1999). This may link to some geophysical data that suggested the presence of sizeable (5×10–15×40 km^2) bodies of magma in the upper mantle (50–90 km in depth) beneath large volcanic centres such as Klyuchevskoy, Koryasky, Avachinsky and Katmai (Utnasin *et al*. 1975; Matumoto 1971). The combination of high pressures and elevated volatile contents will suppress plagioclase crystallization and the extraction of an assemblage dominated by just olivine and pyroxene ($\pm$ spinel), with or without interaction with peridotitic wall rocks, will result in rapid increases in silica and the transition from basalt to andesite. Magmatic lineages in which indices of assimilation, such as the ^{87}Sr/^{86}Sr ratio, decrease with increasing differentiation (McDermott *et al*. 1993; Heath *et al*. 1998) may well reflect evolution within deep mantle reservoirs through assimilation of old mafic materials.

A working model for the presently available constraints on the time-scales of andesite magma formation, storage and ascent is illustrated on figures 1, 5 and 10. Different elements are distilled off the subducting plate at different places and different times. Elements derived largely from subducted sediment (e.g. Th, REE, Ta, Nb, Zr, Hf, Ti) are added to the mantle wedge 0.3–4 Myr before partial melting. Fluid additions occur much later, and at a relatively constant depth beneath arc volcanoes

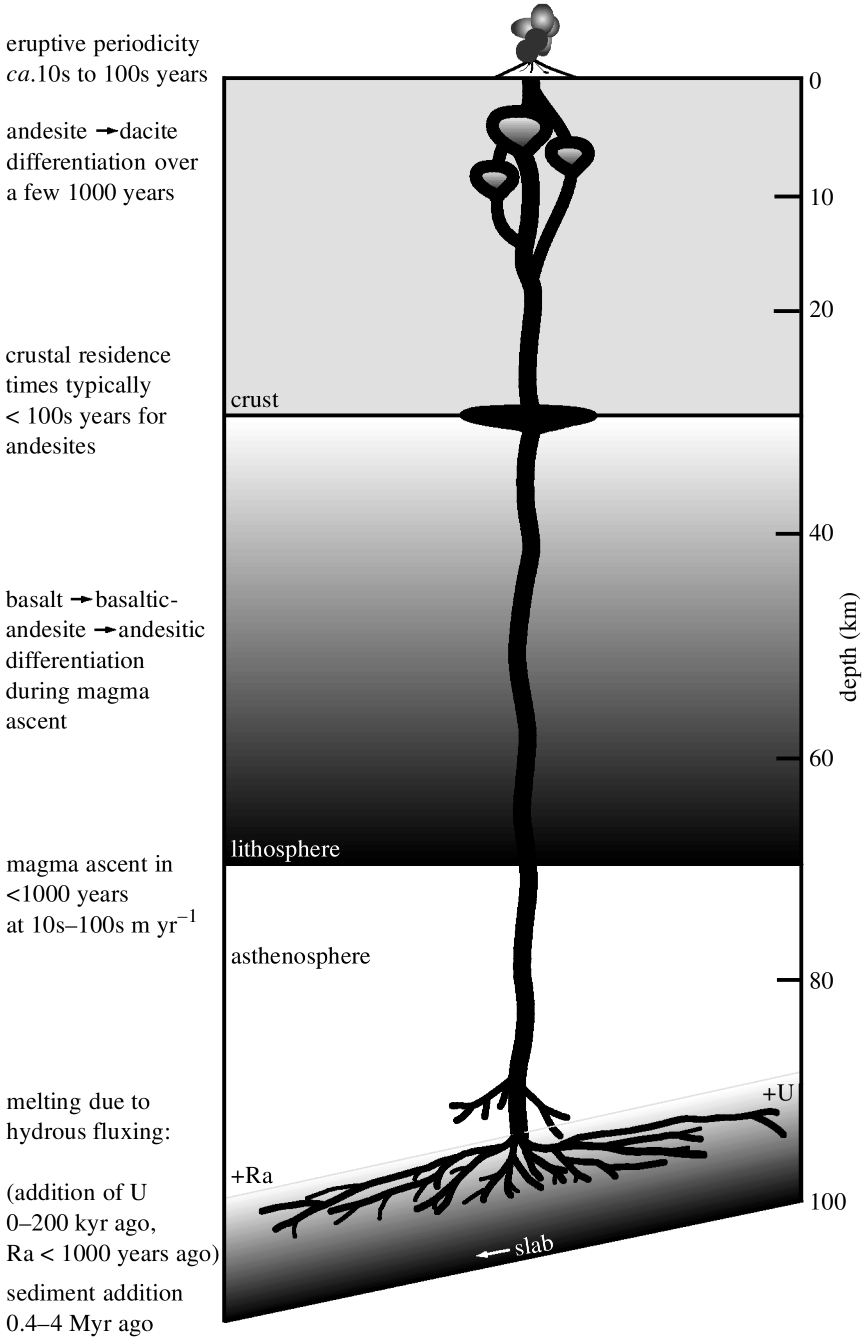

Figure 10. Schematic cross-section of the plumbing and reservoir system for an andesitic volcano modified from Gill (1981) to include element transfer (+U and +Ra are intended to schematically illustrate the spatial and temporal separation of addition of U and Ra due to dehydration reactions in the down-going plate). Magma transport and residence time-scales are discussed in the text.

(Gill 1981), either due to pressure-dependent dehydration reactions (see, for example, Liu *et al.* 1996) or because connectivity in the subducting plate only permits fluid release at a given pressure (Mibe *et al.* 1999). Most fluid mobile elements (e.g. U) are rapidly transferred from the subducting plate to the mantle wedge; however, ^{226}Ra continues to be produced in the plate by residual ^{230}Th, and so ^{226}Ra–^{230}Th disequilibria reflect fluid addition just before partial melting (figure 5). Melting is triggered by fluid addition, but this may be enhanced by a component of decompression melting (Bourdon *et al.* 1999). Fluid-induced melting rates are likely to be high, resulting in a rapid transition from porous to channelled flow and magma ascent rates of tens to hundred of metres per year. Magmatic differentiation from basalt to andesite is also likely to occur rapidly, either during melt transport or during brief periods spent in magma chambers within the lithospheric mantle. The observation of large ^{226}Ra excesses in both basaltic and andesitic magmas demonstrates that the majority of these magmas pass from source to surface in less than a few thousand years. If these rising andesitic magmas pond within the crust, this usually occurs within a few km of the surface where evolution from andesite to dacite occurs via crystal fractionation, with or without combined wall-rock assimilation, on a time-scale typically of the order of 1–8 kyr.

We thank Steve Blake, Jon Davidson, Nick Rogers and Bernard Bourdon for many useful discussions and Peter van Calsteren and Mabs Gilmour for assistance in the laboratories. Constructive reviews by John Eichelberger and Marjorie Wilson did much to improve the manuscript. Simon Turner gratefully acknowledges the support of a Royal Society Research Fellowship and NERC grants GR3/11701 and GR8/03725.

References

Arculus, R. J. 1981 Island arc magmatism in relation to the evolution of the crust and mantle. *Tectonophys.* **75**, 113–133.

Blot, C. 1972 Volcanisme et séismes du manteau supérieur dans l'Archipel des Nouvelles-Hebrides. *Bull. Volcanol.* **36**, 446–461.

Bourdon, B., Turner, S. & Allègre, C. 1999 Melting dynamics beneath the Tonga–Kermadec island arc inferred from ^{231}Pa–^{235}U systematics. *Science* **286**, 2491–2493.

Brenan, J. M., Shaw, H. F., Ryerson, F. J. & Phinney, D. L. 1995 Mineral–aqueous fluid partitioning of trace elements at 900 °C and 2.0 GPa: constraints on the trace element chemistry of mantle and deep crustal fluids. *Geochim. Cosmochim. Acta* **59**, 3331–3350.

Brophy, J. G., Whittington, C. S. & Park, Y.-R. 1999 Sector-zoned augite megacrysts in Aleutian high alumina basalts: implications for the conditions of basalt crystallization and the generation of calc-alkaline series magmas. *Contrib. Mineral. Petrol.* **135**, 277–290.

Cashman, K. V. 1992 Groundmass crystallization of Mount St Helens dacite, 1980–1986: a tool for interpreting shallow magmatic processes. *Contrib. Mineral. Petrol.* **109**, 431–449.

Chabaux, F., Hémond, C. & Allègre, C. J. 1999 ^{238}U–^{230}Th–^{226}Ra disequilibria in the Lesser Antilles arc: implications for mantle metasomatism. *Chem. Geol.* **153**, 171–185.

Condomines, M., Tanguy, J.-C. & Michaud, V. 1995 Magma dynamics at Mt Etna: constraints from U–Th–Ra–Pb radioactive disequilibria and Sr isotopes in historical lavas. *Earth Planet. Sci. Lett.* **132**, 25–41.

Crisp, J. A. 1984 Rates of magma emplacement and volcanic output. *J. Volcanol. Geotherm. Res.* **20**, 177–211.

Davidson, J. P. 1996 Deciphering mantle and crustal signatures in subduction zone magmatism. *Am. Geophys. Union Mono.* **96**, 251–262.

Davidson, J. P. & Tepley, F. J. 1997 Recharge in volcanic systems: evidence from isotope profiles of phenocrysts. *Science* **275**, 826–829.

Davies, J. H. 1999 The role of hydraulic fractures and intermediate-depth earthquakes in generating subduction-zone magmatism. *Nature* **398**, 142–145.

Davies, J. H. & Bickle, M. J. 1991 A physical model for the volume and composition of melt produced by hydrous fluxing above subduction zones. *Phil. Trans. R. Soc. Lond.* A **335**, 355–364.

Davies, J. H. & Stevenson, D. J. 1992 Physical model of source region of subduction zone volcanics. *J. Geophys. Res.* **97**, 2037–2070.

Dvorak, J. J. & Dzurisin, D. 1997 Volcano geodesy: the search for magma reserviors and the formation of eruptive vents. *Rev. Geophys.* **35**, 343–384.

Edwards, B. R. & Russell, J. K. 1998 Time scales of magmatic processes: new insights from dynamic models for magmatic assimilation. *Geology* **26**, 1103–1106.

Eichelberger, J. C. & Westrich, H. R. 1981 Magmatic volatiles in explosive rhyolitic eruptions. *Geophys. Res. Lett.* **8**, 757–760.

Ellam, R. M. & Hawkesworth, C. J. 1988 Is average continental crust generated at subduction zones? *Geology* **16**, 314–317.

Elliott, T., Plank, T., Zindler, A., White, W. & Bourdon, B. 1997 Element transport from slab to volcanic front at the Mariana arc. *J. Geophys. Res.* **102**, 14 991–15 019.

Gardner, J. E., Carey, S., Rutherford, M. J. & Sigurdsson, H. 1995 Petrologic diversity in Mount St Helens dacites during the last 4000 years: implications for magma mixing. *Contrib. Mineral. Petrol.* **119**, 224–238.

George, R. M., Turner, S. P., Hawkesworth, C. J. & Nye, C. 1999 Along-arc U–Th–Ra systematics in the Aleutians. *Eos* **82**, 1023.

Gill, J. B. 1981 *Orogenic andesites and plate tectonics*, pp. 1–390. Springer.

Gill, J. B. & Williams, R. W. 1990 Th isotope and U-series studies of subduction-related volcanic rocks. *Geochim. Cosmochim. Acta* **54**, 1427–1442.

Gill, J. B., Morris, J. D. & Johnson, R. W. 1993 Timescale for producing the geochemical signature of island arc magmas: U–Th–Po and Be–B systematics in recent Papua New Guinea lavas. *Geochim. Cosmochim. Acta* **57**, 4269–4283.

Grove, T. L. & Kinzler, R. J. 1986 Petrogenesis of andesites. *A. Rev. Earth Planet. Sci.* **14**, 417–454.

Halliday, A. N., Fallick, A. E., Dickin, A. P., Mackenzie, A. B., Stephens, W. E. & Hildreth, W. 1983 The isotopic and chemical evolution of Mount St Helens. *Earth Planet. Sci. Lett.* **63**, 241–256.

Halliday, A. N., Mahood, G. A., Holden, P., Metz, J. M., Dempster, T. J. & Davidson, J. P. 1989 Evidence for long residence times of rhyolitic magma in the Long Valley magmatic system: the isotope record in precaldera lavas of Glass Mountain. *Earth Planet. Sci. Lett.* **94**, 274–290.

Hawkesworth, C. J., Turner, S. P., McDermott, F., Peate, D. W. & van Calsteren, P. 1997 U–Th isotopes in arc magmas: implications for element transfer from the subducted crust. *Science* **276**, 551–555.

Heath, E., Turner, S. P., Macdonald, R., Hawkesworth, C. J. & van Calsteren, P. 1997 Long magma residence times at an island arc volcano (Soufrière, St Vincent) in the Lesser Antilles: evidence from ^{238}U–^{230}Th isochron dating. *Earth Planet. Sci. Lett.* **160**, 49–63.

Heath, E., Macdonald, R., Belkin, H., Hawkesworth, C. & Sigurdsson, H. 1998 Magmagenesis at Soufrière volcano, St Vincent, Lesser Antilles arc. *J. Petrol.* **39**, 1721–1764.

Hole, M. J., Saunders, A. D., Marriner, G. F. & Tarney, J. 1984 Subduction of pelagic sediments: implications for the origin of Ce-anomalous basalts from the Mariana islands. *J. Geol. Soc. Lond.* **141**, 453–472.

Hughes, R. D. 1999 The timescales of andesite generation at Mount Ruapehu, New Zealand, p. 317. PhD thesis, The Open University.

Hughes, R. D. & Hawkesworth, C. J. 1999 The effects of magma replenishment processes on ^{238}U–^{230}Th disequilibrium. *Geochim. Cosmochim. Acta* **63**, 4101–4110.

Huppert, H. E. & Sparks, R. S. J. 1988 The generation of granitic magmas by intrusion of basalt into continental crust. *J. Petrol.* **29**, 599–624.

Iyer, H. M. 1984 Geophysical evidence for the locations, shapes and sizes, and internal structures of magma chambers beneath regions of Quaternary volcanism. *Phil. Trans. R. Soc. Lond.* A **310**, 473–510.

Jarrard, R. D. 1986 Relations among subduction parameters. *Rev. Geophys.* **24**, 217–284.

Jaupart, C. 1996 Physical models of volcanic eruptions. *Chem. Geol.* **128**, 217–227.

Johnson, M. C. & Plank, T. 1999 Dehydration and melting experiments constrain the fate of subducted sediments. *Geochem. Geophys. Geosys.* **1**. Paper no. 1999 GC000014.

Kay, R. W. 1980 Volcanic arc magmas: implications of a melting–mixing model for element recycling in the crust–upper mantle system. *J. Geol.* **88**, 497–522.

Keppler, H. 1996 Constraints from partitioning experiments on the composition of subduction-zone fluids. *Nature* **380**, 237–240.

Knesel, K. M., Davidson, J. P. & Duffield, W. A. 1999 Evolution of silicic magma through assimilation and subsequent recharge: evidence from Sr isotopes in sanidine phenocrysts, Taylor Creek rhyolite, NM. *J. Petrol.* **40**, 773–786.

La Tourette, T., Hervig, R. L. & Holloway, J. R. 1995 Trace element partitioning between amphibole, phlogopite and basanite melt. *Earth Planet. Sci. Lett.* **135**, 13–30.

Liu, J., Bohlen, S. R. & Ernst, W. G. 1996 Stability of hydrous phases in subducting oceanic crust. *Earth Planet. Sci. Lett.* **143**, 161–171.

McDermott, F. & Hawkesworth, C. 1991 Th, Pb and Sr isotope variations in young island arc volcanics and oceanic sediments. *Earth Planet. Sci. Lett.* **104**, 1–15.

McDermott, F., Defant, M. J., Hawkesworth, C. J., Maury, R. C. & Joron, J. L. 1993 Isotope and trace element evidence for three component mixing in the genesis of the North Luzon arc lavas (Philippines). *Contrib. Mineral. Petrol.* **113**, 9–23.

McKenzie, D. 1985*a* The extraction of magma from the crust and mantle. *Earth Planet. Sci. Lett.* **74**, 81–91.

McKenzie, D. 1985*b* ^{230}Th–^{238}U disequilibrium and the melting process beneath ridge axes. *Earth Planet. Sci. Lett.* **72**, 149–157.

Marsh, B. D. 1987 Petrology and evolution of the N. E. Pacific including the Aleutians. *Pacific Rim Congr.* **87**, 309–315.

Marsh, B. D. 1989 Magma chambers. *A. Rev. Earth Planet. Sci.* **17**, 439–474.

Matumoto, T. 1971 Siesmic body waves observed in the vicinity of Mount Katmai, Alaska, and evidence for the existence of molten chambers. *Geol. Soc. Am. Bull.* **82**, 2905–2920.

Mibe, K., Fujii, T. & Yasuda, A. 1999 Control of the location of the volcanic front in island arcs by aqueous fluid connectivity in the mantle wedge. *Nature* **401**, 259–262.

Miller, D. M., Goldstein, S. L. & Langmuir, C. H. 1994 Cerium/lead and lead isotope ratios in arc magmas and the enrichment of lead in the continents. *Nature* **368**, 514–520.

Morris, J. D., Leeman, B. W. & Tera, F. 1990 The subducted component in island arc lavas: constraints from Be isotopes and B–Be systematics. *Nature* **344**, 31–36.

Nichols, G. T., Wyllie, P. J. & Stern, C. R. 1994 Subduction zone melting of pelagic sediments constrained by melting experiments. *Nature* **371**, 785–788.

Pearce, J. A. & Parkinson, I. J. 1993 Trace element models for mantle melting: application to volcanic arc petrogenesis. *Geol. Soc. Spec. Publ.* **76**, 373–403.

Pickett, D. A. & Murrell, M. T. 1997 Observations of ^{231}Pa/^{235}U disequilibrium in volcanic rocks. *Earth Planet. Sci. Lett.* **148**, 259–271.

Plank, T. & Langmuir, C. H. 1988 An evaluation of the global variations in the major element chemistry of arc basalts. *Earth Planet. Sci. Lett.* **90**, 349–370.

Pyle, D. M. 1992 The volume and residence time of magma beneath active volcanoes determined by decay-series disequilibria methods. *Earth Planet. Sci. Lett.* **112**, 61–73.

Pyle, D. M., Ivanovich, M. & Sparks, R. S. J. 1988 Magma–cumulate mixing identified by U–Th disequilibrium dating. *Nature* **331**, 157–159.

Reagan, M. K., Morris, J. D., Herrstrom, E. A. & Murrell, M. T. 1994 Uranium series and beryllium isotope evidence for an extended history of subduction modification of the mantle below Nicaragua. *Geochim. Cosmochim. Acta* **58**, 4199–4212.

Regelous, M., Collerson, K. D., Ewart, A. & Wendt, J. I. 1997 Trace element transport rates in subduction zones: evidence from Th, Sr and Pb isotope data for Tonga–Kermadec arc lavas. *Earth Planet. Sci. Lett.* **150**, 291–302.

Schaefer, S. J., Sturchio, N. C., Murrell, M. T. & Williams, S. N. 1993 Internal 238U-series systematics of pumice from the November 13, 1985, eruption of Nevado del Ruiz, Columbia. *Geochim. Cosmochim. Acta* **57**, 1215–1219.

Schmidt, M. W. & Poli, S. 1998 Experimentally based water budgets for dehydrating slabs and consequences for arc magma generation. *Earth Planet. Sci. Lett.* **163**, 361–379.

Sigmarsson, O., Condomines, M., Morris, J. D. & Harmon, R. S. 1990 Uranium and ^{10}Be enrichments by fluids in Andean arc magmas. *Nature* **346**, 163–165.

Sisson, T. W. & Bronto, S. 1998 Evidence for pressure-release melting beneath magmatic arcs from basalt at Galunggung, Indonesia. *Nature* **391**, 883–886.

Sparks, R. S. J. 1997 Causes and consequences of pressurisation in lava dome eruptions. *Earth Planet. Sci. Lett.* **150**, 177–189.

Sparks, R. S. J., Sigurdsson, H. & Wilson, L. 1977 Magma mixing: a mechanism of triggering acid explosive eruptions. *Nature* **267**, 315–318.

Sparks, R. S. J., Huppert, H. E. & Wilson, C. J. N. 1990 Comment on 'Evidence for long residence times of rhyolitic magma in the Long Valley magmatic system: the isotope record in precaldera lavas of Glass Mountain' by A. N. Halliday, G. A. Mahood, P. Holden, J. M. Metz, T. J. Dempster and J. P. Davidson. *Earth Planet. Sci. Lett.* **99**, 387–389.

Spiegelman, M. & Elliott, T. 1993 Consequences of melt transport for uranium series disequilibrium in young lavas. *Earth Planet. Sci. Lett.* **118**, 1–20.

Stolper, E. & Newman, S. 1994 The role of water in the petrogenesis of Mariana trough magmas. *Earth Planet. Sci. Lett.* **121**, 293–325.

Tait, S., Jaupart, C. & Vergniolle, S. 1989 Pressure, gas content and eruption periodicity of a shallow, crystallising magma chamber. *Earth Planet. Sci. Lett.* **92**, 107–123.

Tatsumi, Y., Hamilton, D. L. & Nesbitt, R. W. 1986 Chemical characteristics of fluid phase released from a subducted lithosphere and origin of arc magmas: evidence from high-pressure experiments and natural rocks. *J. Volcan. Geotherm. Res.* **29**, 293–309.

Taylor, R. S. & McLennan, S. M. 1981 The composition and evolution of the continental crust: rare earth element evidence from sedimentary rocks. *Phil. Trans. R. Soc. Lond.* A **301**, 381–399.

Turner, S. & Hawkesworth, C. 1997 Constraints on flux rates and mantle dynamics beneath island arcs from Tonga–Kermadec. *Nature* **389**, 568–573.

Turner, S., Hawkesworth, C., van Calsteren, P., Heath, E., Macdonald, R. & Black, S. 1996 U-series isotopes and destructive plate margin magma genesis in the Lesser Antilles. *Earth Planet. Sci. Lett.* **142**, 191–207.

Turner, S., Hawkesworth, C., Rogers, N., Bartlett, J., Worthington, T., Hergt, J., Pearce, J. & Smith, I. 1997 ^{238}U–^{230}Th disequilibria, magma petrogenesis and flux rates beneath the depleted Tonga–Kermadec island arc. *Geochim. Cosmochim. Acta* **61**, 4855–4884.

Turner, S., McDermott, F., Hawkesworth, C. & Kepzhinskas, P. 1998 A U-series study of Kamchatka: constraints on source composition and melting conditions. *Contrib. Mineral. Petrol.* **133**, 217–234.

Turner, S. P., Peate, D. W., Hawkesworth, C. J., Eggins, S. M. & Crawford, A. J. 1999 Two mantle domains and the time scales of fluid transfer beneath the Vanuatu arc. *Geology* **27**, 963–966.

Turner, S., Bourdon, B., Hawkesworth, C. & Evans, P. 2000 ^{226}Ra–^{230}Th evidence for multiple dehydration events and rapid melt ascent beneath the Tonga–Kermadec island arc. *Earth Planet. Sci. Lett.* (In the press.)

Utnasin, V. K., Abdurakhimov, A. I., Anasov, G. I., Balesta, S. T., Budyanskiy, Yu. A., Markhinin, Ye. K. & Fedorenko, V. I. 1975 Deep structure of Klyuchevskoy group of volcanoes and problem of magmatic hearths. *Int. Geol. Rev.* **17**, 791–806.

Volpe, A. M. 1992 ^{238}U–^{230}Th–^{226}Ra disequilibrium in young Mt Shasta andesites and dacites. *J. Volcanol. Geotherm. Res.* **53**, 227–238.

Volpe, A. M. & Hammond, P. E. 1991 ^{238}U–^{230}Th–^{226}Ra disequilibrium in young Mt St Helens rocks: time constraint for magma formation and crystallization. *Earth Planet. Sci. Lett.* **107**, 475–486.

Wolff, J. A., Ramos, F. C. & Davidson, J. P. 1999 Sr isotope disequilibrium during differentiation of the Bandelier Tuff: constraints on the crystallization of a large rhyolitic magma chamber. *Geology* **27**, 495–498.

Zellmer, G. F., Blake, S., Vance, D., Hawkesworth, C. & Turner, S. 1999 Plagioclase residence times at two island arc volcanoes (Kameni islands, Santorini, and Soufrière, St Vincent) determined by Sr diffusion systematics. *Contrib. Mineral. Petrol.* **136**, 345–357.

Zellmer, G., Turner, S. & Hawkesworth, C. 2000 Timescales of destructive plate margin magmatism: new insights from Santorini, Aegean volcanic arc. *Earth Planet. Sci. Lett.* **174**, 265–281.